Graphene field emission devices

S. Kumar, G. S. Duesberg, R. Pratap, and S. Raghavan

Citation: Applied Physics Letters **105**, 103107 (2014); doi: 10.1063/1.4895022
View online: http://dx.doi.org/10.1063/1.4895022
View Table of Contents: http://scitation.aip.org/content/aip/journal/apl/105/10?ver=pdfcov
Published by the AIP Publishing

Graphene field emission devices

S. Kumar,[1,a)] G. S. Duesberg,[2] R. Pratap,[1,3] and S. Raghavan[1]
[1]*Centre for Nanoscience and Engineering, Indian Institute of Science, Bengaluru, India*
[2]*Centre for Research on Adaptive Nanostructures and Nanodevices (CRANN) and School of Chemistry, Trinity College Dublin, Dublin, D2, Ireland*
[3]*Department of Mechanical Engineering, Indian Institute of Science, Bengaluru, India*

(Received 12 May 2014; accepted 25 August 2014; published online 11 September 2014)

Graphene field emission devices are fabricated using a scalable process. The field enhancement factors, determined from the Fowler-Nordheim plots, are within few hundreds and match the theoretical predictions. The devices show high emission current density of $\sim$10 nA μm^{-1} at modest voltages of tens of volts. The emission is stable with time and repeatable over long term, whereas the noise in the emission current is comparable to that from individual carbon nanotubes emitting under similar conditions. We demonstrate a power law dependence of emission current on pressure which can be utilized for sensing. The excellent characteristics and relative ease of making the devices promise their great potential for sensing and electronic applications. © *2014 AIP Publishing LLC*.
[http://dx.doi.org/10.1063/1.4895022]

The development of new types of sensors from emerging materials is one of the most exciting fields of nanotechnology. There is an enormous need for the development of energy efficient sensors for electronic systems, medical, and mobile technologies. Among numerous approaches, field emission (FE) in micro-devices can be used for tracking nanoscale motion as well as surface modifications,[1–6] both of which are fundamental techniques for building efficient and versatile sensors. In fact, the most precise nanomechanical mass sensor demonstrated[7] used FE from an individual carbon nanotube (CNT) as sensing signal. CNTs, as graphitic nano-carbons, have proven to be the best materials for FE,[8] as they make sharp emitters, are chemically and mechanically very stable, and are among best conductors of heat and electricity. However, a scalable process for precise selection and placement CNTs has not surfaced yet. Graphene, on the other hand, has all the benefits of CNTs and is compatible with thin film processing. It has low mass density, large surface to volume ratio, and can be functionalized with myriad moieties, all of which can make it very sensitive to external influence. With these properties, graphene field emission devices (GFEDs) hold great promise for sensing as well as high performance electronics and display technology.

Surprisingly, there have been no attempts at implementation of GFEDs. So far FE from graphene has only been reported for flakes of graphene lying on or embedded in a substrate surface[9–13] and for use in display technology. These approaches cannot be directly translated to fabricate well-controlled micro-devices. Ad-hoc experiments have been reported to characterize FE from edges of single edges of graphene,[14–18] which are again of little help in making micro-devices. Lee *et al.*[14] proposed a FED concept, but did not develop the idea.

In this paper, we introduce a well-controlled process flow for making high current, low noise GFEDs which is compatible with semiconductor processing. With chemical vapor deposited (CVD) graphene, we contacted suspended graphene stripes which are separated by a nanoscale gap and characterised FE across it. Arrays of devices were analysed, showing remarkable current densities and noise levels close to FE from CNTs. Their field enhancement factors are as predicted by theory. We demonstrate a power law dependence of emission current on pressure over a large range, which can be used in sensing. The process presented here can also easily be modified to introduce multiple and differently placed electrodes and control gates, modify the surface and change or scale the electrodes. This flexibility will allow fabrication of devices optimised for high performance electronics, displays, and electron sources, as well as of devices made of various other emerging 2D materials.

Graphene was grown by CVD on copper foils following the well established route[19] yielding predominantly monolayer graphene.[20] The transfer of graphene to substrates was done using poly-(methyl-methacrylate) (PMMA) as a support layer. A p-doped Si wafer was wet oxidized to obtain a 300 nm thick silica layer.[20] 30 nm of plasma enhanced CVD SiC was then deposited on the silica layer. Openings were patterned in the SiC layer using e-beam lithography (EBL) and reactive ion etching (RIE). Graphene was transferred on this substrate and patterned by EBL in form of ribbons perpendicular to the openings in SiC layer. Contact pads (10 nm Cr, then 60 nm Au) were deposited on the ends of the ribbons using EBL, sputtering and subsequent lift-off. These steps yielded contacted graphene ribbons lying on top of the thin opening in the SiC layer. A thin layer of PMMA was spin-coated and narrow gaps (50 nm–100 nm) were exposed in it using EBL. The gaps were positioned to cut the graphene ribbons in two halves. Oxygen plasma was used to etch graphene exposed in these gaps to define the two electrodes. PMMA was then removed with acetone. In next step, the substrate was dipped in buffered HF solution to etch the SiO_2 layer exposed in the openings in the SiC layer. Finally, the samples were dried in a critical point drier.

The electrical measurements were carried in high vacuum ($\sim 10^{-6}$ Torr) chamber of an EBL system (Raith Eline) equipped with two nanomanipulators. The nanomanipulators

a)E-mail: shishirk@gmail.com

were connected to a Keithely 2410 C digital source measure unit (SMU), which was controlled by a computer (Fig. 1(c)). Voltages typically lying in range of 0–20 V were used for biasing the devices. The noise floor of the SMU was around 100 pA during measurements. The low vacuum ($\sim 10^{-2}$ Torr) and ambient measurements were done on a Lakeshore vacuum probe station with a rotary pump and a Cascade probe station, respectively. Both the stations used Agilent B1500 system for electrical measurements, which has noise level of 100 fA. Scanning electron microscope (SEM, Carl Zeiss Ultra) images were used to determine the width and length of the nano-gaps in the devices.

SEM images in Fig. 1 show the layouts of a GFED. Two graphene ribbons are suspended on a trench whose walls are made of SiC sitting above SiO_2 and whose bottom is the Si substrate. The ribbons are separated by a nanogap. On applying a bias between the ribbons, electrons are emitted laterally from a ribbon edge (shown by red arrow in Fig. 1(a)). The configuration used here is called lateral FED (LFED) in contrast to vertical FED, which has graphene edges displaced perpendicularly to the substrate. The two configurations are suited for different applications, e.g., vertical FEDs are natural choice for displays. Vertical GFEDs will be reported elsewhere.

The cold field emission emission from a sharp tip is described by the Fowler-Nordheim (FN) equation[21]

$$I = A\varphi^{-1}F^2 \exp\left(-B\varphi^{3/2}/F\right) = A\varphi^{-1}(\beta V/d)^2 \exp\left(-Bd\varphi^{3/2}/\beta V\right) \quad (1)$$

where I is the current density, A (1.54 μA eV V^{-2}) and B (6.83 $eV^{-3/2}$ V nm^{-1}) are known constants, φ is the local work function of the surface and F is the local field. We take I to be linear current density (LCD), which was obtained by dividing the emission current by the length of emission edge. This value is also approximately equal to absolute value of emission current, since the length of emitting edge ranged from 0.5 μm to 1.5 μm. For a given voltage V, the applied macroscopic field is V/d, where d is the gap between the electrodes as measured from the SEM images. The local field is then given by $\beta V/d$, where β is the field enhancement factor due to geometry of the tip. A plot of $\ln(I/F^2)$ against $-1/F$ has a slope $B\varphi^{3/2}/\beta$, from which the values of β (assuming $\varphi \sim 5$ eV) can be extracted. This plot is referred to as a FN plot in the following discussions.

Equation (1) has been derived for point emitters. Recently, Qin *et al.*[22] have derived a modified the FN equation for sheet emitters, which has a factor of $F^{3/2}$ in front of the exponential. The β values obtained using that form are about 10% smaller than those obtained from using the FN equation.[21] We report values obtained from the FN equation below for easier comparison with values in literature.

The *I-F* and FN characteristics of GFEDs measured at 10^{-6} Torr are plotted in Fig. 2. The emission current profiles are symmetric with respect to direction of applied field (Fig. 2(a)), as both the ribbons can emit depending on the bias. The applied bias was below 30 V in all cases. At higher bias dielectric breakdown occurred in underlying SiC/SiO_2 layer near the location where the two ribbons are supported. This limitation has restricted the current densities to tens of nA μm^{-1}. With smaller gaps smaller biases can be used and we expect that current densities can be boosted further. The magnitudes of emission currents from the devices compare favourably with those reported in literature from single graphene edges, e.g., Lee *et al.*[14] ($\sim$10 s of nA), Xiao *et al.*[16] ($\sim$100 pA). A straightforward comparison is not feasible due to different emission setups and lack of edge length data in these reports.

The FN plots of the devices are shown in Fig. 2(b), along with the field enhancement factors determined from the line-fits. The values of β, determined from similar plots, are plotted with respect to the gap between the electrodes in Fig. 2(c). A total of 31 devices were analysed and they have β lying in range of few hundreds, which tend to increase with gap-width between the ribbons. The threshold field E_{th},

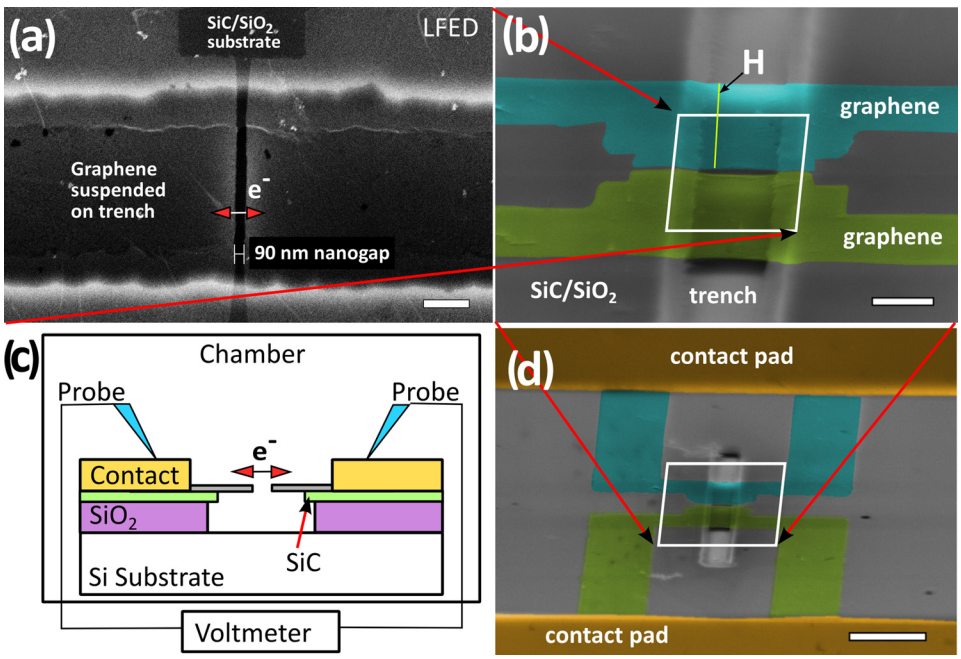

FIG. 1. (a) SEM images of a GFED. The red arrows show flow of electrons in nano-gaps between the electrodes. False colour lower magnification images in (b) and (d) show the layout of the device. The measurement setup in (c) shows the layers used in device stack, starting from Si substrate at the bottom to SiO_2 (300 nm), SiC (30 nm), graphene and contact pads (Cr 10 nm then Au 60 nm). The scale bars are (a) 400 nm, (b) 1 μm, and (d) 5 μm.

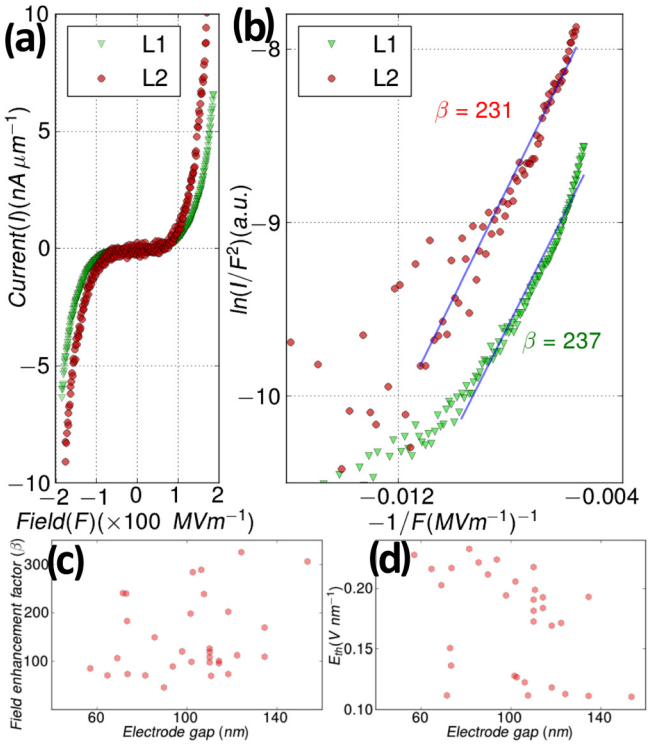

FIG. 2. (a) Typical I-F characteristic of two GFEDs, L1 and L2. (b) FN plot for data shown in (a). The slopes of line-fits were used for determining field enhancement factors β. Scatter plots of (c) field enhancement factors (β) and (d) threshold field E_{th} with respect to gap between the electrodes for 31 LFEDs.

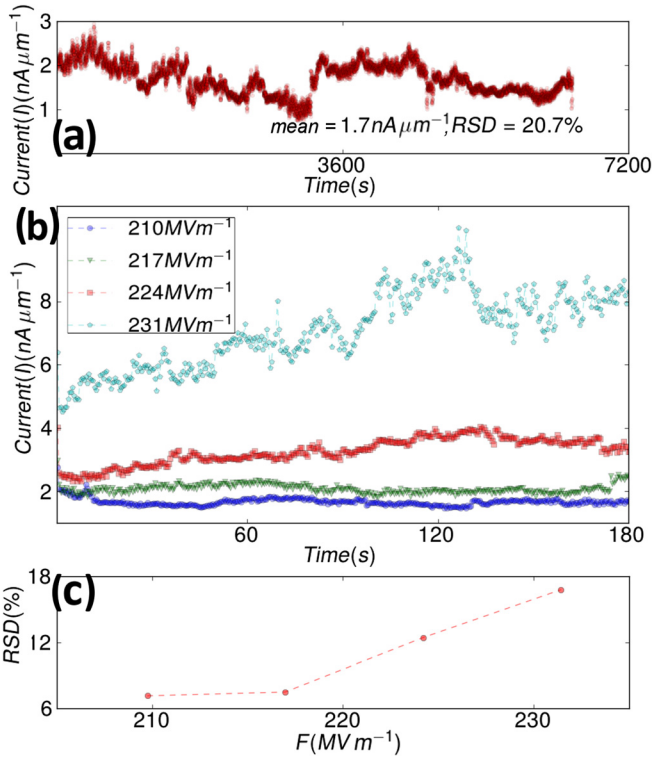

FIG. 3. (a) Field emission current as a function of time for a GFED. The mean current and relative standard deviation (RSD) is also shown. (b) Absolute noise increases with bias as shown in current-time plot for a GFED in (b). The RSD values of these traces have been plotted in (c) showing that the noise increases monotonically with bias and is larger in case of GFEDs.

defined as field needed to obtain 1 nA μm^{-1} current from a device and plotted against gap-width in Fig. 2(d), tends to increase at smaller gap-widths, which is similar to the trend observed by Smith *et al.*[23] in their experiments with ropes of multi-walled CNTs. The reported values of β in literature vary widely, e.g., aggregates of graphene flakes show $\beta \sim 1200$,[9] ~ 5000,[11] $>10\,000$,[12] 5960,[13] and 3517.[14] A better comparison can be made to Bonard *et al.*[24] who measured individual CNTs inside a SEM as we have done for graphene edges. They observed 1 nA current at local fields (i.e., βF) of 3.8 V nm^{-1} and β to be ~ 90. For GFEDs shown, the local fields required for 1 nA current is βE_{th}, which falls in range of 10–30 V nm^{-1}. The values of β for GFEDs are in same range as theirs ($30 \leq \beta \leq 260$ for 40 nanotubes). They showed that the low values of β were accounted for by a model of Edgcombe and Valdrè.[25] Miller *et al.*[26] did a similar calculation for a sheet emitter of height H and thickness $2a$ (0.335 nm for graphene), such that $H \gg 2a$, showing $\beta = (\pi H/4a)^{1/2}$. Using $H = 6\,\mu$m (see Fig. 2(d)), we can calculate β to be ~ 160 for a single ribbon, which is close to the experimental values. The higher local fields required for GFEDs compared to individual CNTs can be attributed to several factors, which include the higher dimensionality of graphene, the presence of trench walls, the unevenness of emitting edge of graphene and the contaminants from processing. Optimisation of fabrication process can reduce the turn-on fields as well as improve the emission stability.

Noise in the emission current is an important consideration in applications because it puts bounds on the device operation range and its robustness. An GFED was monitored for emission for 2 h at a constant bias. The emission current-time plot is shown in Fig. 3(a). The relative standard deviation (RSD) of the emission current comes out to be 20%, a substantial portion of which ($\sim$6%) comes from the noise of the measurement setup which is of the order of 100 pA. The device does show a little drift. However, the measurements done a couple of months apart show almost similar emission characteristics in terms of enhancement factor and noise levels.

The noise levels reported from graphene flakes and measured under similar or better vacuum levels and bias conditions are comparable to what is reported here (10% at 10^{-6} Torr by Soin *et al.*,[27] 20% at 10^{-9} Torr by Huang *et al.*[28]). However, these studies deal with the ensemble averages of an emission current from a large number of flakes, which may distort the characteristics of emission from an individual flake. On the other side is the emission current noise obtained from individual CNT emitters which have much smaller emission edge (few nm) compared to the graphene ribbons studied here. A well controlled study by Jonge *et al.*[29] has shown that the current noise from CNTs can reach 0.02% under UHV (10^{-10} Torr) conditions, but increases to 1%–10% as the vacuum is lowered to 10^{-7} Torr or higher. The reports by Dean and Chalamala[30] (10^{-9} Torr) and Saito and Uemura[31] (10^{-8} Torr) on emission from single CNTs indicate similar or higher current noise.

The source of current noise can be attributed to the addition and release (by impinging ions) of adsorbates on the surface of carbon emitters (NTs, graphite, glassy-carbon, and graphene).[32] The adsorbates change the local potentials,

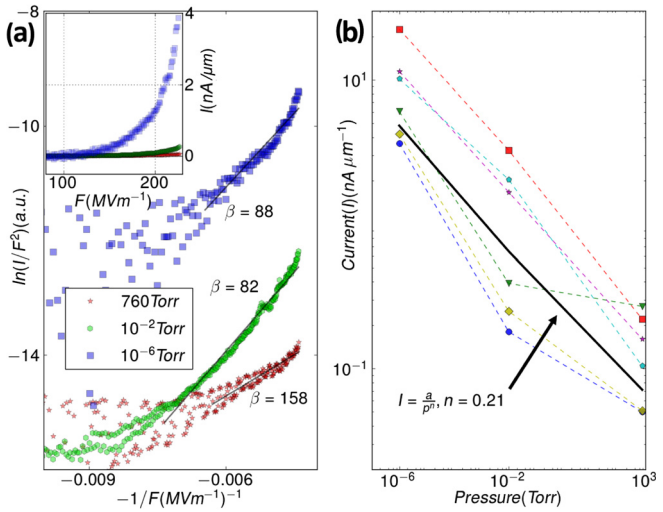

FIG. 4. (a) FN plots for an LFED operating at different pressures. The β values are similar in three cases. The inset shows *I-F* representation of same data. (b) The change in field emission current density for six LFEDs with pressure. The solid line is the fit of $I = ap^{-n}$ to the average of all other lines.

introducing electron traps (e.g., oxygen and water molecules) and scatterers, resulting in reduction of emission current. In other words, the work function φ increases with the presence of adsorbates. The recurring nature of adsorption events produces noise in emission current. At high pressures and fields, the number of adsorption-desorption events increases, which results in larger noise.

The variation of noise with changing electric field is shown in Fig. 3(b) for a device operated for 3 min for each of the different biases. The change in RSD of emission current is easily seen, and is plotted in Fig. 3(c). As expected, the noise levels show a monotonic increase with increasing bias. As noted earlier a substantial portion of noise is due to instrumentation, this is seen in the relative relatively flat noise for lower biases (Fig. 3(c)). A better noise immunity will be achieved with smaller nano-gaps, which will yield higher emission currents at lower fields.

Fig. 4(a) shows the emission characteristics of a device at the pressure values corresponding to vacuum created by a turbomolecular pump, by a roughing pump and in ambient. Although the field enhancement factor β remains similar in three cases, the emission current drops and the noise increases with increase in pressure as is visible in the FN plots. These observations are consistent with increased occurrence of adsorption of oxygen and water on the edge and basal planes of graphene ribbons. The noise shown for the high vacuum case (10^{-6} Torr) is dominated by the noise from the measurement setup.

Fig. 4(b) shows the response of 6 GFEDs under these measurement conditions. The emission current values were picked up from the I-F characteristic of the GFEDs at the highest bias applied (~20 V), which was same for all devices. We see a clear decrease in the current with pressure and a remarkable uniformity in response from all the devices. The linear behavior on the log-log plot indicates a power-law relationship between the emission current and pressure, $I = ap^{-n}$. A fit shows that $n = 0.21$. Kim and Lee[33] observed $n = 0.335$ in their experiments on field emission from vertical ZnO nanowires under variable pressures. The difference in the values of n could be due to the difference in geometry and adsorption kinetics. The change in emission current can be used to sense changes in pressure. Although the range of pressures that can be sensed is large, a larger emission current and lower noise should improve the sensing performance, which can be achieved using smaller gaps between the electrodes.

In conclusion, we have demonstrated the fabrication and operation of GFEDs using CVD graphene. These devices show emission currents densities in range of 10 s of nA μm^{-1} at modest bias voltages of tens of volts. The enhancement factors (few hundreds) and noise in emission current (~10%) are similar to those reported for single CNT field emitters. Application in pressure sensing was demonstrated by simply tracking change in emission current with pressure. Improvement in processing, e.g., decrease in nano-gap dimension will lead to even higher performance. Such devices will not only enable nanoscale motion and chemical sensing but also help applications in electronics and fundamental studies of 2D materials.

We thank Professor N. Bhat and Professor A. Naik for discussion and Professor S. Mohan for lending some instruments. S.K. thanks Sangeeth Kallat and Manikant Singh for help in fabrication and measurement setup, respectively. This work was partially supported by the SFI under Contract Nos. 12/RC/2278 and PI_10/IN.1/I3030. The work was carried out at the National Nanofabrication Centre and Micro-Nano Characterization Facility of CeNSE, IISc.

[1]C. K. Yang, A. J. le Fèbre, G. Pandraud, E. van der Drift, and P. J. French, J. Vac. Sci. Technol., B **26**, 927 (2008).
[2]Y. D. Lee, W.-S. Cho, S.-I. Moon, Y.-H. Lee, J. K. Kim, S. Nahm, and B.-K. Ju, Chem. Phys. Lett. **433**, 105 (2006).
[3]W. Wen, L. Wang, J. Gao, and D. Sun, in *Proceedings of 2nd IEEE International Conference on Nano/Micro Engineered and Molecular Systems, NEMS'*07 (2007), p. 199.
[4]K. Qian, T. Chen, B. Yan, Y. Lin, D. Xu, Z. Sun, and B. Cai, Electron. Lett. **41**, 824 (2005).
[5]I.-M. Choi and S.-Y. Woo, Appl. Phys. Lett. **87**, 173104 (2005).
[6]S. T. Purcell, P. Vincent, C. Journet, and V. T. Binh, Phys. Rev. Lett. **89**, 276103 (2002).
[7]K. Jensen, K. Kim, and A. Zettl, Nat. Nanotechnol. **3**, 533 (2008).
[8]J.-M. Bonard, H. Kind, T. Stöckli, and L.-O. Nilsson, Solid-State Electron. **45**, 893 (2001).
[9]G. Eda, H. Emrah Unalan, N. Rupesinghe, G. A. J. Amaratunga, and M. Chhowalla, Appl. Phys. Lett. **93**, 233502 (2008).
[10]Z. Wu, S. Pei, W. Ren, D. Tang, L. Gao, B. Liu, F. Li, C. Liu, and H. Cheng, Adv. Mater. **21**, 1756 (2009).
[11]A. Malesevic, R. Kemps, A. Vanhulsel, M. P. Chowdhury, A. Volodin, and C. Van Haesendonck, J. Appl. Phys. **104**, 084301 (2008).
[12]U. A. Palnitkar, R. V. Kashid, M. A. More, D. S. Joag, L. S. Panchakarla, and C. N. R. Rao, Appl. Phys. Lett. **97**, 063102 (2010).
[13]T. Hallam, M. T. Cole, W. I. Milne, and G. S. Duesberg, Small **10**, 94 (2014).
[14]S. Lee, S. S. Lee, and E.-H. Yang, Nanoscale Res. Lett. **4**, 1218 (2009).
[15]H. M. Wang, Z. Zheng, Y. Y. Wang, J. J. Qiu, Z. B. Guo, Z. X. Shen, and T. Yu, Appl. Phys. Lett. **96**, 023106 (2010).
[16]Z. Xiao, J. She, S. Deng, Z. Tang, Z. Li, J. Lu, and N. Xu, ACS Nano **4**, 6332 (2010).
[17]X. Wei, D. Golberg, Q. Chen, Y. Bando, and L. Peng, Nano Lett. **11**, 734 (2011).
[18]S. Srisonphan, Y. S. Jung, and H. K. Kim, Nat. Nanotechnol. **7**, 504 (2012).
[19]X. Li, W. Cai, J. An, S. Kim, J. Nah, D. Yang, R. Piner, A. Velamakanni, I. Jung, E. Tutuc, S. K. Banerjee, L. Colombo, and R. S. Ruoff, Science **324**, 1312 (2009).

[20]See supplementary material at http://dx.doi.org/10.1063/1.4895022 for Raman and SEM characterization of CVD graphene, detailed process steps and for analysis using modified FN equation.
[21]H. Fowler and L. Nordheim, Proc. R. Soc. London, Ser. A **119**, 173 (1928).
[22]X.-Z. Qin, W.-L. Wang, N.-S. Xu, Z.-B. Li, and R. G. Forbes, Proc. R. Soc. A **467**, 1029 (2011).
[23]R. C. Smith, R. D. Forrest, J. D. Carey, W. K. Hsu, and S. R. P. Silva, Appl. Phys. Lett. **87**, 013111 (2005).
[24]J.-M. Bonard, K. A. Dean, B. F. Coll, and C. Klinke, Phys. Rev. Lett. **89**, 197602 (2002).
[25]C. J. Edgcombe and U. Valdrè, J. Microsc. **203**, 188 (2001).
[26]R. Miller, Y. Y. Lau, and J. H. Booske, Appl. Phys. Lett. **91**, 074105 (2007).
[27]N. Soin, S. Sinha Roy, S. Roy, K. S. Hazra, D. S. Misra, T. H. Lim, C. J. Hetherington, and J. A. McLaughlin, J. Phys. Chem. C **115**, 5366 (2011).
[28]C.-K. Huang, Y. Ou, Y. Bie, Q. Zhao, and D. Yu, Appl. Phys. Lett. **98**, 263104 (2011).
[29]N. de Jonge, M. Allioux, J. T. Oostveen, K. B. K. Teo, and W. I. Milne, Appl. Phys. Lett. **87**, 133118 (2005).
[30]K. A. Dean and B. R. Chalamala, Appl. Phys. Lett. **75**, 3017 (1999).
[31]Y. Saito and S. Uemura, Carbon **38**, 169 (2000).
[32]S. Yamamoto, S. Hosoki, S. Fukuhara, and M. Futamoto, Surf. Sci. **86**, 734 (1979).
[33]D.-H. Kim and H.-R. Lee, J. Korean Phys. Soc. **45**, L803 (2004).